Stability of Slopes in Cohesive-Frictional Soil

A. ASSADI
M.Sc., Ph.D.
Res. Assoc., Dept. of Civ. Engrg. and Surveying, Univ. of Newcastle, Australia
S.W. SLOAN
M.Sc., Ph.D.
Sr. Lect., Dept. of Civ. Engrg. and Surveying, Univ. of Newcastle, Australia

SUMMARY This paper examines the drained stability of slopes in cohesive-frictional soil. Plane strain conditions are assumed and active failure is achieved by increasing either the unit weight of the material or the boundary pressure applied at the top surface. Two numerical methods are described which are based on the limit theorems of classical plasticity and a finite element discretisation. These methods give solutions which are rogorous upper and lower bounds on the exact collapse load.In the lower bound procedure, statically admissible stress fields are computed by using an internal linear approximation to the Mohr-Coulomb yield criterion. Conversely, in the upper bound procedure, kinematically admissible velocity fields are computed using an external approximation to the Mohr-Coulomb yield criterion. Both of the methods lead to large linear programming problems. The results show that the true collapse load is bracketted within two reasonable bounds which are tighter than existing analytical solutions.

1. INTRODUCTION

The plane strain slope problem to be considered is shown in Figure 1. The soil is modelled as a Mohr-Coulomb material with a uniform effective cohesion c, friction angle ϕ and unit weight γ . Collapse of the slope may occur in a variety of ways. For a fixed slope height H, collapse may be triggered by increasing either surcharge σ_s or the unit weight γ. The drained stability of the slope is thus conveniently described by the dimensionless load parameters $\gamma H/c$ and σ_s/c.

This paper describes the application of two numerical techniques to yield sharp bounds on $\gamma H/c$ or σ_s/c for drained conditions. The numerical schemes are based on a finite element formulation of the plastic limit theorems and lead to large linear programming problems. Safe estimates for the value of $\gamma H/c$ or σ_s/c may be obtained using the lower bound theorem of classical plasticity which states that any statically admissible stress field will provide a lower bound on the true limit load. Unsafe estimates for the value of $\gamma H/c$ or σ_s/c can be deduced from the upper bound theorem which states that any kinematically admissible velocity field will provide an upper bound on the true limit load. The exact value of $\gamma H/c$ or σ_s/c may thus be bounded from above and below but the bounds must be sufficiently tight to be of practical use.

One of the first to propose the lower bound theorem as a linear programming problem was Lysmer (1). Similar methods have also been described by Anderheggen and Knopfel (2), Bottero et al. (3), Sloan (4) and Assadi and Sloan (5). A key development, due to Pastor (6), was the introduction of extension elements which permit statically admissible stress fields to be extended to semi-infinite domains. Another important improvement, due to Sloan (7), was the development of an active set algorithm, which fully exploits sparsity and uses a steepest edge search to locate the optimal solution rapidly.

One of the earliest investigations of a numerical formulation for the upper bound theorem may be found in Anderheggen and Knopfel (2). Bottero et al. (3) included the effects of

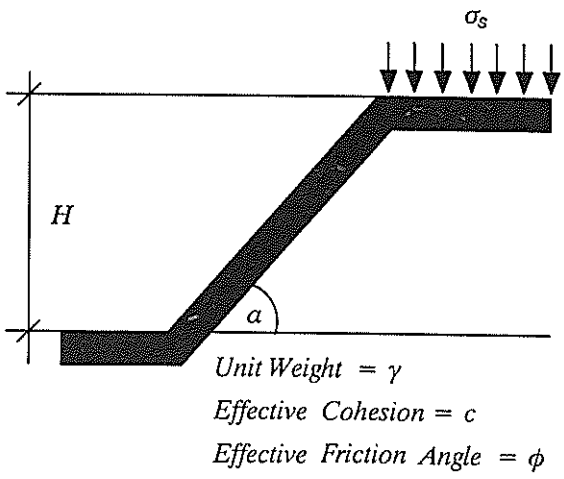

Figure 1 Plane strain slope

velocity discontinuities and applied the method to a variety of soil mechanics problems. Sloan (8) proposed a formulation based on duality theory and used the steepest edge active set algorithm to solve the resulting linear programming problem efficiently. The upper bound method, like the lower bound method, typically leads to very large optimisation problems involving several thousand variables and constraints, and it is essential to exploit the extreme sparsity of the constraint matrix to the full.

2. FINITE ELEMENT FORMULATION OF THE LOWER BOUND THEOREM

2.1 Elements for Lower Bound Limit Analysis

The sign conventions for stresses, with compression taken as positive, are shown in Figure 2. The formulation employs three types of elements as shown in Figure 3. The stresses vary linearly within each element according to

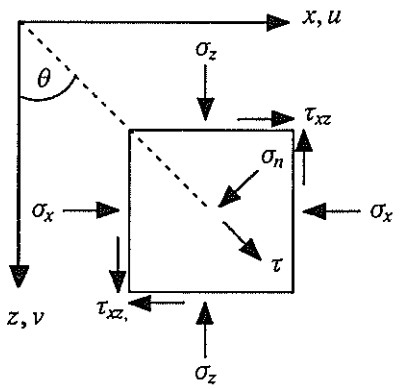

Figure 2 Sign convention for velocities and stresses

$$\sigma_x = \sum_{i=1}^{i=3} N_i \sigma_{xi} \;\; ; \;\; \sigma_z = \sum_{i=1}^{i=3} N_i \sigma_{zi} \;\; ; \;\; \tau_{xz} = \sum_{i=1}^{i=3} N_i \tau_{xzi} \quad (1)$$

where N_i are linear shape functions and σ_{xi}, σ_{zi},τ_{xzi} are the nodal stresses. The triangular and rectangular extension elements, which enable a statically admissible stress field to be extended within a semi-infinite domain, are based on the same linear expansion as the simple three noded triangle.

Stress discontinuities are permitted to occur at all edges that are shared by adjacent elements.

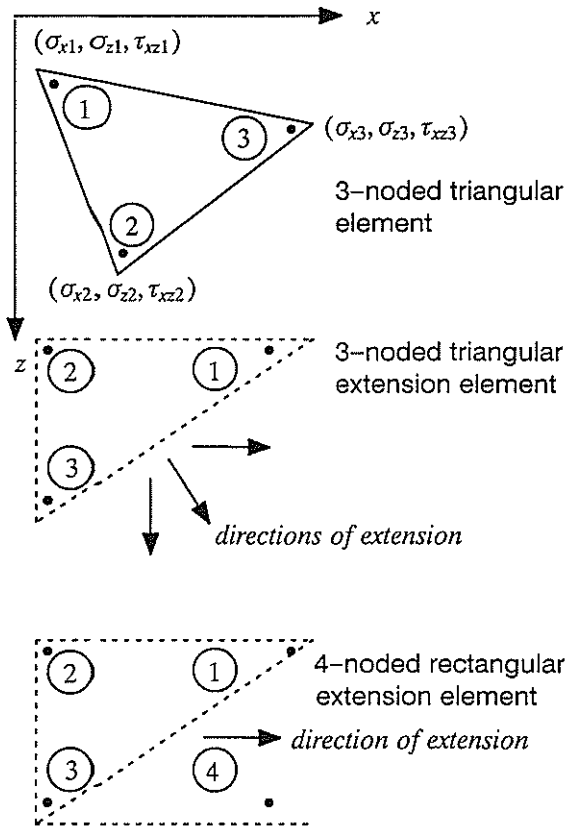

Figure 3 Elements for lower bound limit analysis

2.2 Statically admissible stress field

In order to be statically admissible, and thus provide a rigorous lower bound on the collapse load, the stresses must be in equilibrium, satisfy the stress boundary conditions, and nowhere violate the yield criterion. These conditions are treated as linear constraints which are expressed in terms of the unknown nodal stresses and body forces. The collapse load is described by an objective function which is either a function of the unknown normal boundary stresses or the unknown body forces.

2.3 Equilibrium Conditions

Under plane strain conditions the equilibrium equations may be written as

$$\frac{\partial \sigma_x}{\partial x} + \frac{\partial \tau_{xz}}{\partial z} = 0 \quad ; \quad \frac{\partial \sigma_z}{\partial z} + \frac{\partial \tau_{xz}}{\partial x} = \gamma \quad (2)$$

Differentiating equation (1) and inserting in equation (2), two linear constraints are obtained

$$\mathbf{a}_1 \quad \mathbf{x} \quad = \quad \mathbf{b}_1 \quad (3)$$

with $\mathbf{a}_1$ a constant matrix, $\mathbf{x} = \{\sigma_{x1}, \sigma_{z1}, \tau_{xz1},\ldots,\sigma_{x3}, \sigma_{z3}, \tau_{xz3}\}^T$ and $\mathbf{b}_1 = \{0, \gamma\}^T$.

For each rectangular extension element, three additional linear equalities(one for each component of stress) are necessary to extend the linear stress distribution to the fourth node. These have the matrix form of

$$\mathbf{a}_2 \quad \mathbf{x} \quad = \quad \mathbf{b}_2 \quad (4)$$

where $\mathbf{x} = \{\sigma_{x1}, \sigma_{z1}, \tau_{xz1},\ldots,\sigma_{x4}, \sigma_{z4}, \tau_{xz4}\}^T$ and $\mathbf{b}_2 = \{0,0,0,0\}^T$.

A stress discontinuity is statically admissible if all pairs of nodes on opposite sides of the discontinuity have equal shear and normal stresses. This will give rise to four equality constraints and may be written in terms of the nodal stresses according to

$$\mathbf{a}_3 \quad \mathbf{x} \quad = \quad \mathbf{b}_3 \quad (5)$$

where $\mathbf{a}_3$ is a constant matrix, $\mathbf{x} = \{\sigma_{x1}, \sigma_{z1}, \tau_{xz1},\ldots,\sigma_{x4}, \sigma_{z4}, \tau_{xz4}\}^T$ and $\mathbf{b}_3 = \{0,0,0,0\}^T$.

2.4 Stress Boundary Conditions

The prescribed stress boundary conditions on the external faces of the domain, may be treated as equality constraints on the nodal stresses. If an edge is defined by the nodes (1,2), and the stresses at these nodes are prescribed to be (σ_{n1}, τ_1) and (σ_{n2}, τ_2), then substitution into the stress transformation equations leads to four equality constraints of the form

$$\mathbf{a}_4 \quad \mathbf{x} \quad = \quad \mathbf{b}_4 \quad (6)$$

where
$\mathbf{a}_4$ is a constant matrix, $\mathbf{x} = \{\sigma_{x1}, \sigma_{z1}, \tau_{xz1}, \sigma_{x2}, \sigma_{z2}, \tau_{xz2}\}^T$ and $\mathbf{b}_4 = \{\sigma_{n1}, \tau_1, \sigma_{n2}, \tau_2\}^T$.

Equations (3), (4), (5) and (6) ensure that the stress field satisfies equilibrium and the boundary conditions and the remaining step is to enforce linear constraints to satisfy the yield conditions.

2.5 Internal Linear Approximation to Yield Criterion

Under plane strain loading, the Mohr-Coulomb yield criterion may be written as

$$F = (\sigma_x - \sigma_z)^2 + (2\tau_{xz})^2 - ((\sigma_x + \sigma_z)\sin\phi + 2c\cos\phi)^2 \quad (7)$$

and we require that $F \leq 0$.

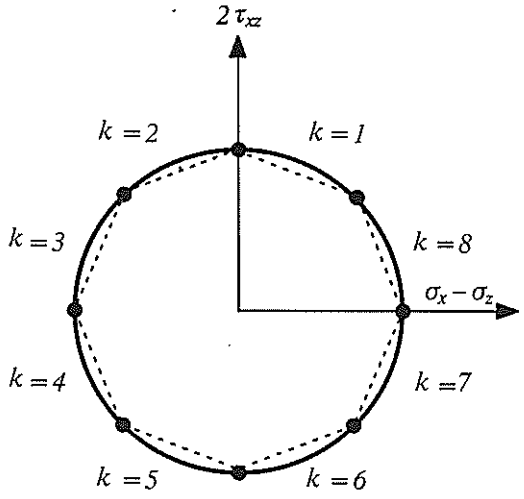

Figure 4 Internal linearization of Mohr-Coulomb yield criterion

In terms of the quantities $(\sigma_x - \sigma_z)$ and $2\tau_{xz}$, this function plots as a circle of radius $((\sigma_x+\sigma_z)\sin\phi+2c\cos\phi)$ as shown in figure 4. Since this type of constraint is nonlinear, it is replaced by an inscribed polygon with p sides of equal length. With reference to Figure 4, which shows an eight-sided approximation, the linearised yield criterion is given by

$$F_k = A_k\sigma_x + B_k\sigma_z + C_k\tau_{xz} - 2c\cos\phi\cos(\pi/p) \leq 0 \quad (8)$$

where
$A_k = \cos(2\pi k/p) - \sin\phi\cos(\pi/p), B_k = -\cos(2\pi k/p) - \sin\phi\cos(\pi/p), C_k = 2\sin(2\pi k/p)$ and k ranges from 1 to p. The above equation needs to be enforced at each node of each triangular element. For each rectangular extension element the inequality constraints $F_{k1} \leq F_{k2}$, $F_{k2} \leq 0$ and $F_{k3} \leq 0$ have to be imposed. In each three-noded triangular extension element we need to apply the constraints $F_{k1} \leq F_{k2}$, $F_{k3} \leq F_{k2}$ and $F_{k2} \leq 0$. In general terms, the linearised yield criterion generates inequalities of the form

$$\mathbf{a}_5 \quad \mathbf{x} \quad \leq \quad \mathbf{b}_5 \quad (9)$$

where $\mathbf{a}_5$ is comprised of the coefficients A_k, B_k, C_k, $\mathbf{x} = \{\sigma_{xi}, \sigma_{zi}, \tau_{xzi}\}^T$ and $\mathbf{b}_5 = 2c\cos\phi\cos(\pi/p)\{1,1,...,1\}^T$.

2.6 Objective Function

To isolate the particular stress field which optimises the collapse load, an objective function has to be defined. The objective function can be expressed as an integral of the form

$$Q = \int_s \sigma_n ds \quad (10)$$

where Q is the collapse load per unit thickness and σ_n is the normal stress acting over some part of the external boundary. For each segment on the boundary, we have

$$Q = (L/2)(\sigma_{n1} + \sigma_{n2}) \quad (11)$$

where L is the length of the segment and $(\sigma_{n1}, \sigma_{n2})$ are the normal stresses at each of its ends. Q may be expressed in terms of the cartesian nodal stresses of Figure 2 according to

$$Q \quad = \quad \mathbf{c}^T \quad \mathbf{x} \quad (12)$$

where the coefficients $\mathbf{c}$ are functions of the length and orientation of the boundary edge, and $\mathbf{x} = \{\sigma_{x1}, \sigma_{z1}, \tau_{xz1}, \sigma_{x2}, \sigma_{z2}, \tau_{xz2}\}^T$.

2.7 Computation of Lower Bound Collapse Load

Once the various coefficients are assembled, the problem of finding a statically admissible stress field, which maximises the collapse load over a specified area, may be written as

$$\begin{array}{ll} \textit{Minimise} & -\mathbf{C}^T\mathbf{X} \\ \\ \textit{Subject to} & \mathbf{A}_1\mathbf{X} = \mathbf{B}_1 \\ & \mathbf{A}_2\mathbf{X} = \mathbf{B}_2 \\ & \mathbf{A}_3\mathbf{X} = \mathbf{B}_3 \\ & \mathbf{A}_4\mathbf{X} = \mathbf{B}_4 \\ & \mathbf{A}_5\mathbf{X} \leq \mathbf{B}_5 \end{array} \quad (13)$$

where $\mathbf{X}$ is the global vector of unknown stresses and $\mathbf{C}^T\mathbf{X}$ corresponds to the collapse load.

3. FINITE ELEMENT FORMULATION OF THE UPPER BOUND THEOREM

3.1 Elements for Upper Bound Limit Analysis

The triangular element which is used to model the velocity field is shown in Figure 5. The velocities vary linearly within each element according to

$$u = \sum_{i=1}^{i=3} N_i u_i \quad ; \quad v = \sum_{i=1}^{i=3} N_i v_i \quad (14)$$

where N_i are linear shape functions and (u_i, v_i) are the nodal velocities in the x and z directions respectively. A kinematically admissible velocity field must satisfy the flow rule and the velocity boundary conditions.

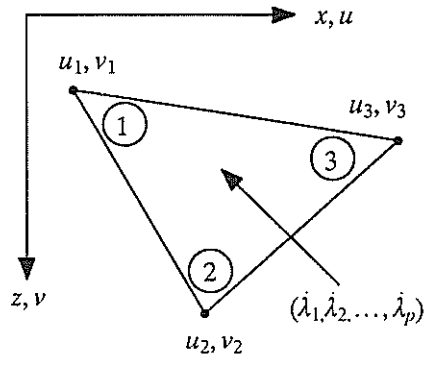

Figure 5 Element for upper bound limit analysis

3.2 Flow Rule Equations

For plane strain deformation, the flow rule equations are given by

$$\dot{\varepsilon}_x = \dot{\lambda}\frac{\partial F}{\partial \sigma_x} \; ; \; \dot{\varepsilon}_z = \dot{\lambda}\frac{\partial F}{\partial \sigma_z} \; ; \; \dot{\gamma}_{xz} = \dot{\lambda}\frac{\partial F}{\partial \tau_{xz}} \qquad (15)$$

where $\dot{\lambda} \geq 0$ is a plastic multiplier rate and compressive strains are taken as positive.

To remove the stress terms from the flow rule equations, and thus provide a linear relationship between the unknown velocities and plastic multiplier rates, an external linear approximation to the Mohr-Coulomb yield criterion is needed.

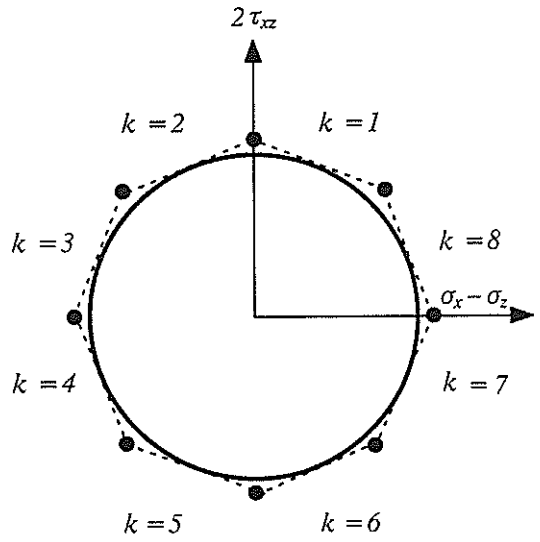

Figure 6 External linearization of Mohr–Coulomb yield criterion

3.3 External Linear Approximation to Yield Criterion

An eight-sided approximation is shown in Figure 6. This polygon has p sides of equal length and the linearised yield condition may be written as

$$F_k = A_k\sigma_x + B_k\sigma_z + C_k\tau_{xz} - 2c\cos\phi = 0 \qquad (16)$$

where
$A_k = \cos(2\pi k/p) - \sin\phi$, $B_k = -\cos(2\pi k/p) - \sin\phi$, $C_k = 2\sin(2\pi k/p)$ and k ranges from 1 to p. Differentiating equation (14) and using equations (15) and (16) furnishes the flow rule equations as

$$\begin{aligned}
&\sum_{i=1}^{i=3}\frac{\partial N_i}{\partial x}u_i + \sum_{k=1}^{k=p}\dot{\lambda}_k A_k = 0 \\
&\sum_{i=1}^{i=3}\frac{\partial N_i}{\partial z}v_i + \sum_{k=1}^{k=p}\dot{\lambda}_k B_k = 0 \quad \dot{\lambda}_k \geq 0 \qquad (17)\\
&\sum_{i=1}^{i=3}\frac{\partial N_i}{\partial x}v_i + \sum_{i=1}^{i=3}\frac{\partial N_i}{\partial z}u_i + \sum_{k=1}^{k=p}\dot{\lambda}_k C_k = 0
\end{aligned}$$

These relations may be expressed in the general form of

$$\mathbf{a}_{11}\mathbf{x}_1 + \mathbf{a}_{12}\mathbf{x}_2 = \mathbf{b}_1 \qquad (18)$$

where $\mathbf{a}_{11}$ and $\mathbf{a}_{12}$ are matrices of constants, $\mathbf{b}_1 = \{0,0,0\}^T$, $\mathbf{x}_1 = \{u_1, v_1, u_2, v_2, u_3, v_3\}^T$, and $\mathbf{x}_2 = \{\dot{\lambda}_1, ..., \dot{\lambda}_p\}^T$.

3.4 Velocity Discontinuity

For each velocity discontinuity one inequality constraint is required to ensure that the power dissipated along the discontinuity is nonnegative. The sign of each discontinuity,s, refers to the sense of the tangential jump in the velocity, u_t, and is defined so that $\mid u_t \mid = su_t$, where $s = \pm 1$ and is specified as data. The constraint $su_t \geq 0$, may be written as

$$\mathbf{a}_2 \; \mathbf{x}_1 \leq \mathbf{b}_2 \qquad (19)$$

where $\mathbf{a}_2$ is a function of the discontinuity orientation and direction of sliding s, $\mathbf{x}_1 = \{u_1, v_1, u_2, v_2\}^T$ and $\mathbf{b}_2 = 0$.

To satisfy the flow rule condition in a discontinuity an equality constraint is enforced to ensure that the angle between the discontinuity and the direction of the velocity jump is equal to ϕ. This may be expressed as

$$\mathbf{a}_3 \; \mathbf{x}_1 = \mathbf{b}_3 \qquad (20)$$

in which $\mathbf{a}_3$ is a function of the discontinuity orientation, direction of sliding and ϕ, $\mathbf{x}_1 = \{u_1, v_1, u_2, v_2\}^T$ and $\mathbf{b}_3 = 0$.

3.5 Velocity Boundary Conditions

The boundary conditions on the velocities give rise to constraints of the general form

$$\mathbf{a}_4 \; \mathbf{x}_1 = \mathbf{b}_4 \qquad (21)$$

where $\mathbf{a}_4$ is a matrix of constants, $\mathbf{x}_1 = \{u_i, v_i\}^T$ for node i and $\mathbf{b}_4$ is a vector of prescribed values.

3.6 Computation of Upper Bound Collapse Load

Once the various coefficients are assembled the problem of finding a kinematically admissible velocity field, which minimises the total dissipated power, may be expressed as

$$\begin{aligned}
&\textit{Minimise} && \mathbf{C}_1^T\,\mathbf{X}_1 + \mathbf{C}_2^T\,\mathbf{X}_2 \\
&\textit{Subject to} && \mathbf{A}_{11}\,\mathbf{X}_1 + \mathbf{A}_{12}\,\mathbf{X}_2 = \mathbf{B}_1 \\
& && \mathbf{A}_2\,\mathbf{X}_1 \leq \mathbf{B}_2 \\
& && \mathbf{A}_3\,\mathbf{X}_1 = \mathbf{B}_3 \\
& && \mathbf{A}_4\,\mathbf{X}_1 = \mathbf{B}_4 \\
& && \mathbf{X}_2 \geq 0
\end{aligned} \qquad (22)$$

where $\mathbf{X}_1$ is the global vector of unknown velocities, $\mathbf{X}_2$ is the global vector of unknown plastic multiplier rates, $\mathbf{C}_1^T\,\mathbf{X}_1$ is the power dissipated by plastic shearing in the velocity discontinuities, and $\mathbf{C}_2^T\,\mathbf{X}_2$ is the power dissipated by plastic deformation in the triangles. A detailed analysis of various strategies for solving this type of optimisation problem efficiently may be found in Sloan (8). We note in passing that equation (22) may be solved very efficiently by applying the steepest edge active set algorithm to its dual.

4. RESULTS

A typical lower bound mesh, for $\alpha = 45$, $\sigma_s/c = 0$ and $\phi = 20$ is shown in Figure 7. The grid has 1170 nodes, 356 triangles, 2 triangular extension elements, 24 rectangular extension elements and 562 stress discontinuities and was

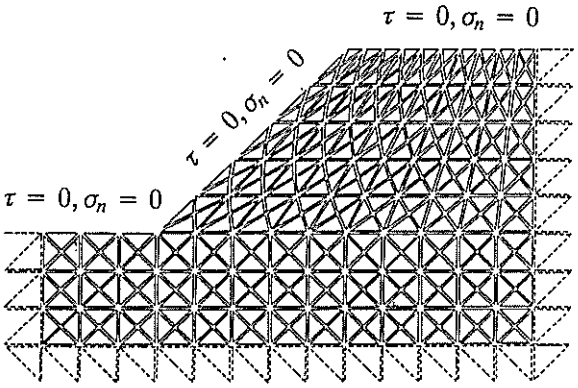

Figure 7 Lower bound mesh for nonvertical slope with $\alpha = 45$, $\sigma_s/c = 0$ and $\phi = 20$

adopted after experimenting with a wide variety of arrangements. The configuration of the extension elements ensures that the stress field can be extended throughout the semi-infinite domain of the problem, without violating equilibrium, the stress boundary conditions or the yield criterion, and thus provides a rigorous lower bound on the collapse load. To perform the lower bound computation, we first prescribe values for H, α,σ_s, c, and ϕ and then solve equation (13) to find a statically admissible stress field which maximises a uniform unit weight for the slope. For a 12-sided approximation to the Mohr-Coulomb yield surface, the mesh of Figure 7 gives a lower bound of $\gamma H/c = 15.74$.

A typical upper bound mesh, also for the case of $\alpha = 45$, $\sigma_s/c = 0$ and $\phi = 20$ is shown in Figure 8. The grid has two vertical and two horizontal discontinuities and the boundary conditions are as shown. Overall, there are 391 nodes and 620 triangles. To compute an upper bound for $\gamma H/c$, we first select values for H, α,σ_s, c, and ϕ and then solve equation (22) to find a kinematically admissible velocity field which minimises a uniform unit weight for the section. For the mesh of Figure 8, with a 12-sided approximation to the yield surface and the same properties as before, the upper bound method furnishes a value for $\gamma H/c$ of 18.30.

Figure 9 shows the stability bounds for a slope with $\alpha = 45$ and $\phi = 0$ in which two extreme points on each bound have been connected by a straight line.

Figures 10 and 11 illustrate a complete summary of the stability bounds for $\alpha = 90$ and a range of ϕ from 0 to 50.

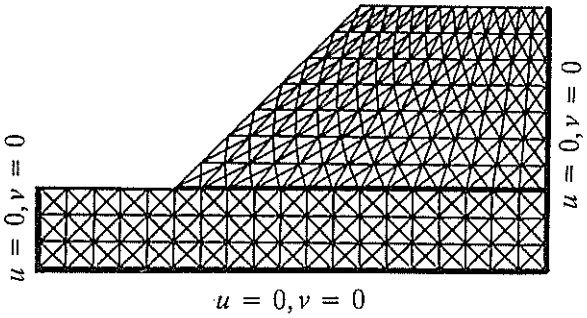

Figure 8 Upper bound mesh for nonvertical slope with $\alpha = 45$, $\sigma_s/c = 0$ and $\phi = 20$

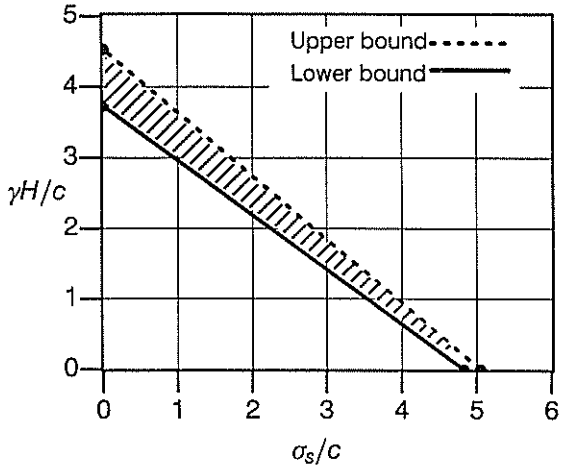

Figure 9 Stability bounds for nonvertical slope problem with $\alpha = 45$ and $\phi = 0$

5. CONCLUSIONS

The drained stability of a slope, under conditions of plane strain, has been investigated. Rigorous bounds on $\gamma H/c$ and σ_s/c using numerical formulation of the limit theorems, have enabled the exact solution to be bracketted within quite close bounds for a range of slope geometries.

6. ACKNOWLEDGEMENTS

The research reported in this paper is funded by a grant from the Australian Research Council. The authors are thankful for this support.

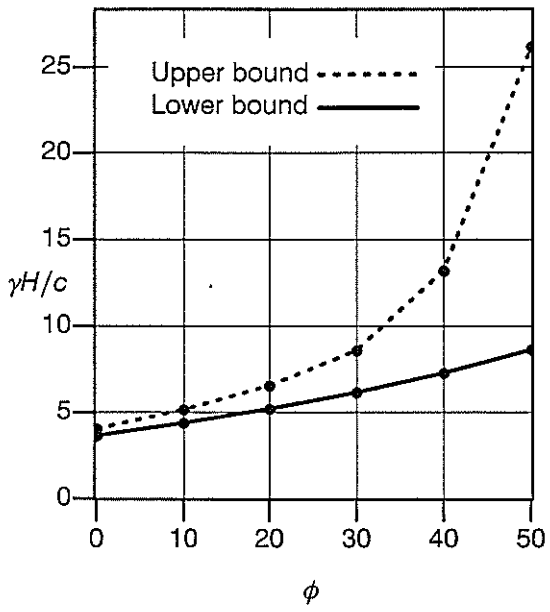

Figure 10 Stability bounds for vertical slope with $\sigma_s/c = 0$

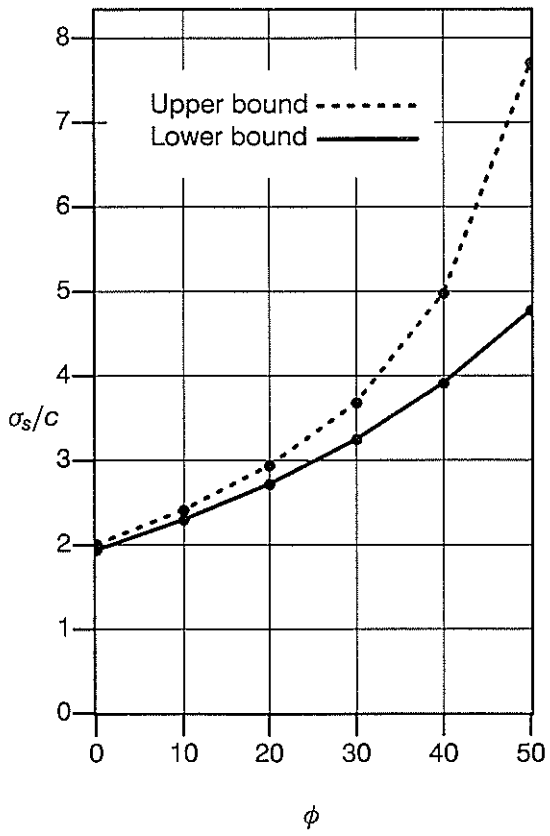

Figure 11 Stability bounds for vertical slope with $\gamma H/c = 0$

7. REFERENCES

1. Lysmer,J. "Limit Analysis of Plane problems in Soil Mechanics", Journal of Soil Mechanics and Foundation Division,A.S.C.E.,Vol. 96,SM4,1311-1334, 1970.

2. Anderheggen,E.,Knopfel,H. "Finite Element Limit Analysis Using Linear Programming", International Journal of Solids and Structures,No. 8, 1413-1431, 1972.

3. Bottero,A.,Negre,R.,Pastor,J.,Turgeman,S. "Finite Element Method and Limit Analysis Theory for Soil Mechanics Problems", Computer Methods in Applied Mechanics and Engineering,No. 22, 131-149, 1980.

4. Sloan,S.W. "Lower Bound Limit Analysis Using Finite Elements and Linear Programming", International Journal for Numerical and Analytical Methods in Geomechanics, No. 12, 61-77, 1988.

5. Assadi,A.,Sloan,S.W. "Undrained Stability of A Shallow Square Tunnel", Journal of Geotechnical Engineering A.S.C.E., Vol. 117, No. 8, 1152-1173, 1991.

6. Pastor,J. "Limit Analysis :Numerical Determination of Complete Statical Solutions-Application to Vertical Cut", Journal de Mechanique Appliquee(in French),No. 2, 167-196, 1978.

7. Sloan,S.W. " A Steepest Edge Active Set Algorithm for Solving Sparse Linear Programming Problems", International Journal for Numerical Methods in Engineering, No. 26, 2671-2685, 1988.

8. Sloan,S.W. "Upper Bound Limit Analysis Using Finite Elements and Linear Programming", International Journal for Numerical and Analytical Methods in Geomechanics, No. 13, 263-282.